STRATEGIES FOR LAVA TUBE DETECTION WITH GRAIL DATA L. Chappaz[1], H. J. Melosh[1,2], K. C. Howell[1],and the GRAIL mission team. [1]School of Aeronautics and Astronautics, Purdue University, West Lafayette, Indiana 47907-2045, 2Earth, Atmospheric and Planetary Science, Purdue University, West Lafayette, Indiana 47907-2051..

Introduction: The success of the NASA's GRAIL mission–a twin spacecraft formation revolving around the moon in a quasi-circular polar orbit–now provides the highest resolution and most accurate gravity data for the Moon. The low altitude at which some of this data was collected in the GRAIL extended mission (down to ca. 6 km over the lunar surface) potentially allows the detection of small-scale surface or subsurface features. We have focused on the specific task of detecting the presence and extent of empty lava tubes beneath the mare surface. In addition to their importance for understanding the emplacement of the mare flood basalts, open lava tubes are of interest as possible habitation sites safe from cosmic radiation and micrometeorite impacts [1]. The existence of such natural caverns is now supported by Kaguya's discoveries of deep pits in the lunar mare [2].

In this investigation, a first stage of the analysis is to develop tools to best exploit the rich gravity data toward the numerical detection of these small features. At the time of the writing of this abstract, only the data collected during the nominal phase of the mission is available. The extended phase of the mission is characterized by much lower altitude passages over the lunar surface and is anticipated to provide even higher resolution data. Two independent strategies are considered: one based on gradiometry techniques and a second one that relies on cross-correlation of individual tracks.

Gradiometry: The first strategy relies on the numerical inspection of the lunar gravitational potential, computed from a set of spherical harmonics that is truncated and tapered to some predeterminded degree and order to magnify the short wave length structures of interest. Fron any gridded scalar field, a widely employed method to detect or highlight ridges or valleys within the field of interest involves the computation of the hessian and consequently the eigenvalues and eigenvectors that are associated with the hessian of the scalar field. In essence, the eigenvalue of largest magnitude and the corresponding eigenvector are associated with the direction of maimum gradient in the field. In this investigation, similar to [3], eigenvalue maps that depict the magnitude of the largest magnitude eigenvalue for each point on a grid on the lunar surface are produced from the numerical computation of the hessian and eigenvalues of the potential field. Note that there are a few possible variations. Either the Free-air potential or the potential corrected for topography and terrain can be employed in the analysis, depending on the objective. Also, both angular (longitude-latitude) or spatial (distance) can be employed to evaluate the numerical derivatives. A sample eigenvalue map generated from the Bouguer gravitational potential, that is, including a correction for topography and terrain, computed using spherical harmonic coefficients from degree and order 50 to 300, and filtered with a cosine taper over 20 degrees and orders is illustrated in Figure 1. The color scale represents the signed magnitude of the largest magnitude eigenvalue of the Hessian of the gravitational potential with derivatives evaluated using spatial quantities.

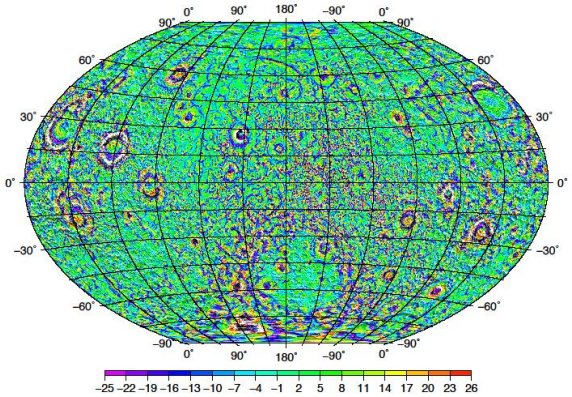

Fig. 1: Eigenvalue map: largest eigenvalues of Hessian of the Bouguer potential.

For the purpose of this analysis, rather then global maps that represent the entire lunar surface, very localized maps that focus on specific regions are more relevant. Consider a region in the Aristharcus plateau that contains Aristachus crater and one of the largest known lunar rilles, Shroeder's Valley. Figure 2 illustrates the correspoinding local eigenvalue maps, with all four combinations for Free-air/Bouguer potential and spatial/angular derivatives, overlaid with the local topography from LOLA. From these local maps, it is not evident that the structures that emerge from these maps do, in fact, correspond to the presence of the rille. Although not included in this abstract, a sensitivity analysis on the truncation and tapering of the harmonic coefficients reveals that these structures are consistent, in general, but do experience variations.

Cross-Correlation: Another strategy relies on exploiting directly the KBRR track data, that is, the relative acceleration of the two spacecraft as they travel on their respectice orbit. Only the horizontal component of the relative acceleration is directly available from the

measurements, in contrast to the radial (i.e. vertical) or lateral components. From either the vertical or horizontal acceleration component, simple analytical expressions describe the acceleration anomaly the spacecraft would experience as it flies perpendicularly over an infinitely long lava tube just beneath the surface that is idealized as an empty horizontal cylinder.

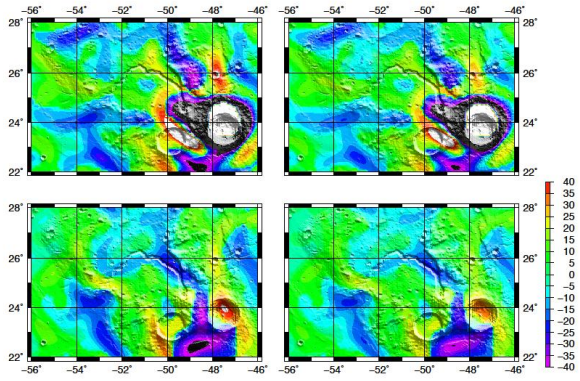

Fig.2: Local eigenvalues map in the Shroder Valley region with topography overlaid.

Figure 3 illustrates the horizontal and vertical acceleration sensed by the GRAIL spacecraft assuming an empty cylinder of diameter 1 km overflown at 50 km, the average altitude for the nomial mission, and 20 km, the corresponding average altitude for the extended mission.

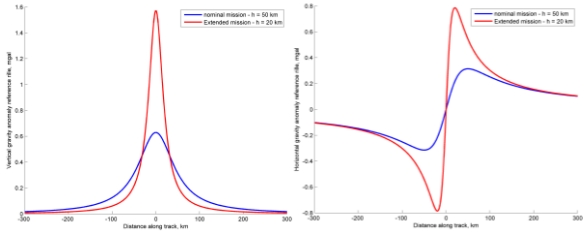

Fig.3: Analytical vertical (left) and horizontal (right) gravity anomaly.

These relations can be employed to construct a reference signal for the structures to be detected, that is, the lava tubes. Then, a mathematical construct in the form of the cross-correlation is employed between a reference signal and the KBRR signal. For practical considerations, only a reduced portion of the track data is employed at once. Track data is subvided into individual tracks that corresponds to a longitude and a range of latitude. Also, to exploit the assumed linearity of the lava tube, several tracks for a set of neighboring discrete longitudes are included in the same computation. Figure 4 illustrates a proof of concept of this idea. This figure is constructed from the cross-correlation between 15 individual tracks that correspond to artificial data created from the readily available GRAIL gridded vertical Bouguer gravity data set for longitudes between 304^o and 312^o with each track spanning latitudes from 10 to 30^o, and a reference signal constructed assuming a 5 km altitude and 2 km diameter lava tube. As a validation tool, a noisy reference signal is also embedded within a discrete subset of tracks to simulate the passage of the spacecraft over some fictious structure. On each vertical line in the figure, the color represents the value of the cross-correlation coefficients, from dark blue to red. The higher the value of the coefficients, and positive, the better the portion of the track data resembles the reference signal, as the the cross-correlation operates as a matching filter.

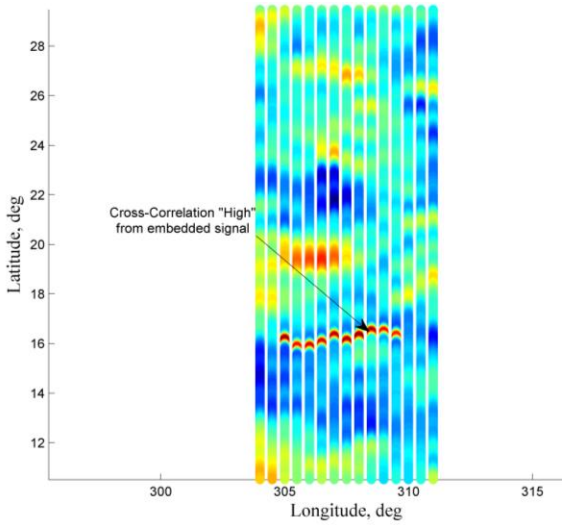

Fig.4: Cross-correlation profile for track data.

The artificially embedded rille signal clearly appears on the cross-correlation profile reprentation as a narrow, pseudo-linear red trace.

Conclusions: At this time, only the data from the nominal phase of the mission is available and the tools to exploit the KBRR data are still being developed. However, preliminary simulations indicate that even with the unprecedented accuracy of the GRAIL gravity reduction, the gradiometry approach does not seem to yield decisive results. The second strategy based on cross-correlation is promising. A combination of both strategies, in addition to exploiting the data from the extended mission–expected to have a significant accuracy improvement–is the main avenue of research for the further development of tools to detect and identify small structures such as lava tubes beneath the lunar mare.

References: [1] De Angelis et al. (2001) BAAS 33, 1037. [2] Haruyama et al. (2009), GRL 36, L21206. [3] Hanna et al. (2012) Science DOI:10.1126/science.1231753 .